

Article

Synthesis, *in vitro* Evaluation and Radiolabelling of Fluorinated Puromycin Analogues: Potential Candidates for PET Imaging of Protein Synthesis.

Helen M. Betts, Selena Milicevic Sephton, Carmen Tong, Ramla O. Awais, Philip J. Hill, Alan C. Perkins, and Franklin I. Aigbirhio

J. Med. Chem., **Just Accepted Manuscript** • DOI: 10.1021/acs.jmedchem.6b00968 • Publication Date (Web): 03 Oct 2016

Downloaded from <http://pubs.acs.org> on October 4, 2016

Just Accepted

“Just Accepted” manuscripts have been peer-reviewed and accepted for publication. They are posted online prior to technical editing, formatting for publication and author proofing. The American Chemical Society provides “Just Accepted” as a free service to the research community to expedite the dissemination of scientific material as soon as possible after acceptance. “Just Accepted” manuscripts appear in full in PDF format accompanied by an HTML abstract. “Just Accepted” manuscripts have been fully peer reviewed, but should not be considered the official version of record. They are accessible to all readers and citable by the Digital Object Identifier (DOI®). “Just Accepted” is an optional service offered to authors. Therefore, the “Just Accepted” Web site may not include all articles that will be published in the journal. After a manuscript is technically edited and formatted, it will be removed from the “Just Accepted” Web site and published as an ASAP article. Note that technical editing may introduce minor changes to the manuscript text and/or graphics which could affect content, and all legal disclaimers and ethical guidelines that apply to the journal pertain. ACS cannot be held responsible for errors or consequences arising from the use of information contained in these “Just Accepted” manuscripts.

1
2
3
4
5
6
7
8
9
10
11
12
13
14
15
16
17
18
19
20
21
22
23
24
25
26
27
28
29
30
31
32
33
34
35
36
37
38
39
40
41
42
43
44
45
46
47
48
49
50
51
52
53
54
55
56
57
58
59
60

Synthesis, *in vitro* Evaluation and Radiolabelling of Fluorinated Puromycin Analogues: Potential Candidates for PET Imaging of Protein Synthesis

Helen M. Betts^{†*}, *Selena Milicevic Sephton*^{‡§*}, *Carmen Tong*[¶], *Ramla O. Awais*[#], *Philip J. Hill*^{||}, *Alan C. Perkins*[#], *Franklin I. Aigbirhio*[§].

[†] Nottingham University Hospitals NHS Trust, PET/CT Center, Nottingham City Hospital, Hucknall Road, Nottingham, NG5 1PB, UK.

[§] Molecular Imaging Chemistry Laboratory, Wolfson Brain Imaging Center, University of Cambridge, Cambridge, CB2 0QQ, UK.

[¶] School of Life Sciences, University of Nottingham, University Park, Nottingham, NG7 2RD, UK.

[#] Radiological Sciences, School of Medicine, University of Nottingham, Queen's Medical Center, Derby Road, Nottingham, NG7 2UH, UK.

^{||} School of Biosciences, University of Nottingham, Sutton Bonington Campus, Sutton Bonington, LE12 5RD, UK.

KEYWORDS Positron emission tomography; protein synthesis; puromycin; fluorine-18;

ABSTRACT

There is currently no ideal radiotracer for imaging protein synthesis rate (PSR) by positron emission tomography (PET). Existing fluorine-18 labelled amino acid-based radiotracers predominantly visualize amino acid transporter processes, and in many cases they are not incorporated into nascent proteins at all. Others are radiolabelled with the short half-life positron emitter carbon-11 which is rather impractical for many PET centers. Based on the puromycin (**6**) structural manifold, a series of 10 novel derivatives of **6** was prepared *via* Williamson ether synthesis from a common intermediate. A bioluminescence assay was employed to study their inhibitory action on protein synthesis which identified fluoroethyl analogue (**7b**) as a lead compound. The fluorine-18 analogue was prepared *via* nucleophilic substitution of the corresponding tosylate precursor in modest radiochemical yield $2\pm 0.6\%$ and excellent radiochemical purity ($>99\%$) and showed complete stability over 3 h at ambient temperature.

INTRODUCTION

Protein translation is a fundamental process for function and survival of all organisms. Enzymes, membrane receptors, structural proteins, growth factors amongst many more are constantly produced within the cell under tight control.¹ Disruption of cellular protein synthesis indicates disease, characterized for instance by an increase of the rate of protein synthesis in malignant growth, or by a reduction in rate in certain neurodegenerative disorders.^{2,3} The ability to visualize protein synthesis rate (PSR) is therefore an important goal in diagnosis, treatment and monitoring of these conditions. Positron emission tomography (PET) is an ideal technique

1
2
3 with which to do this. Since PET requires sub-nanomolar concentrations of radiolabelled tracer
4
5 molecules, cellular processes such as PSR can be probed without causing a pharmacological
6
7 effect.⁴ Several amino acids labelled with positron emitters have been investigated to this end,
8
9 although their application in PSR imaging has several critical limitations. Carbon-11 labelled
10
11 methionine and leucine ($[^{11}\text{C}]\mathbf{1}$, $[^{11}\text{C}]\text{MET}$ and $[^{11}\text{C}]\mathbf{2}$, $[^{11}\text{C}]\text{LEU}$, Figure 1) are used for imaging
12
13 PSR, but the short physical half-life of carbon-11 (20 min) makes their use practically
14
15 impossible at PET scanning centers without a cyclotron, severely limiting their accessibility.^{5,6}
16
17 Furthermore, $[^{11}\text{C}]\mathbf{1}$ produces brain-penetrating radiolabelled metabolites.⁶ Fluorine-18 ($t_{1/2} =$
18
19 110 min) labelled analogues such as *S*-(3- $[^{18}\text{F}]$ fluoropropyl)homocysteine ($[^{18}\text{F}]\mathbf{3}$,
20
21 $[^{18}\text{F}]\text{FPHCYS}$) and *O*-(2- $[^{18}\text{F}]$ fluoroethyl)tyrosine ($[^{18}\text{F}]\mathbf{4}$, $[^{18}\text{F}]\text{FET}$), are not recognized by the
22
23 cellular protein synthesis mechanism, and therefore report amino acid active uptake, rather than
24
25 PSR.^{7,8} The tyrosine analogue 2- $[^{18}\text{F}]$ fluorotyrosine ($[^{18}\text{F}]\mathbf{5}$, $[^{18}\text{F}]\text{FTYR}$), is incorporated into
26
27 nascent proteins, but in addition to its challenging electrophilic radiosynthesis via $[^{18}\text{F}]\text{F}_2$ gas
28
29 rather than $[^{18}\text{F}]\text{F}^-$, the resulting PET images are also dominated by the amino acid transporter
30
31 processes.⁸ (Figure 1). A new fluorine-18 labelled radiotracer capable of imaging PSR is
32
33 therefore required.
34
35
36
37
38
39
40
41
42
43
44
45
46
47
48
49
50
51
52
53
54
55
56
57
58
59
60

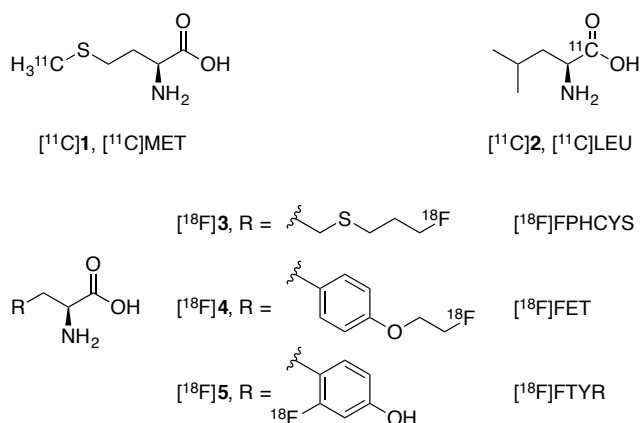


Figure 1. Selected carbon-11 and fluorine-18 amino acid radiotracers.

The aim of this project was to develop a novel radiotracer which: (1) enables measurement of PSR *in vivo*; (2) is not an amino acid and thus does not participate in the amino acid active transport mechanism; and (3) is radiolabelled with fluorine-18, via $[\text{F}^{18}]\text{fluoride}$.

Puromycin (**6**, PURO, Figure 2) is an aminonucleoside antibiotic that inhibits protein synthesis in both bacteria and eukaryotes by mimicking aminoacyl-tRNA (**8**) at the ribosome.^{9,10}

Compound **6** and some structural analogues, enter the ribosomal site A and form an amide bond with the C-terminus of a nascent protein, thus anchoring at sites of active protein growth.⁹

Studies have demonstrated that **6** can be used directly to assess ribosome mediated peptide bond formation since it does not require soluble translation factors for function, it does not induce EF-Tu-GTPase activity and it can enter the ribosome independently.¹¹⁻¹⁴ Furthermore, incorporation of **6** into newly synthesized protein has been established as a direct readout of translation rate, by comparison with classical $[\text{S}^{35}]\text{MET}$ studies.¹⁵ Fluorescent analogues of **6** have been successfully used to monitor protein synthesis (PS) in tissue samples (*ex vivo*)¹⁶ and scandium-44, gallium-68 and carbon-11 radiolabelled **6** derivatives have been described for PET.^{11,17,18} However, the scandium-44 and gallium-68 complexes are structurally dominated by

the metal chelate, and carbon-11 radiolabelled **6** is limited by the short physical half-life of the radionuclide. We hypothesized that a fluorinated analogue of **6** would be a preferable radiotracer for PET imaging, as well as incorporating a more widely available radioisotope. The literature precedent demonstrates that derivatives of **6** modified at the phenyl ring retain the inhibitory activity of the parent,^{13,16,19} which prompted us to investigate the effect of introduction of a fluorine atom into the scaffold of **6** by varying functional groups at the phenol as point of modification (**7b-k**, Figure 2). We also considered potential routes for facile introduction of fluorine-18 in this position using a nucleophilic approach. Herein, we report the synthesis of several derivatives of **6**, their ability to inhibit PS, as well as the radiolabelling of the most prominent derivative as a potential PET radiotracer.

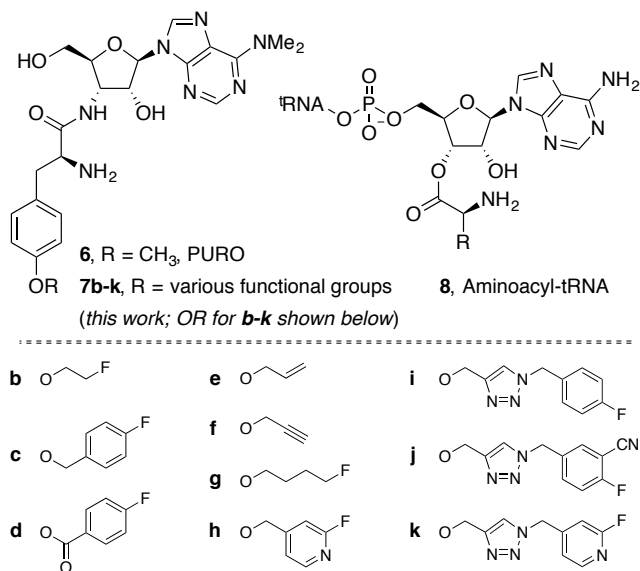
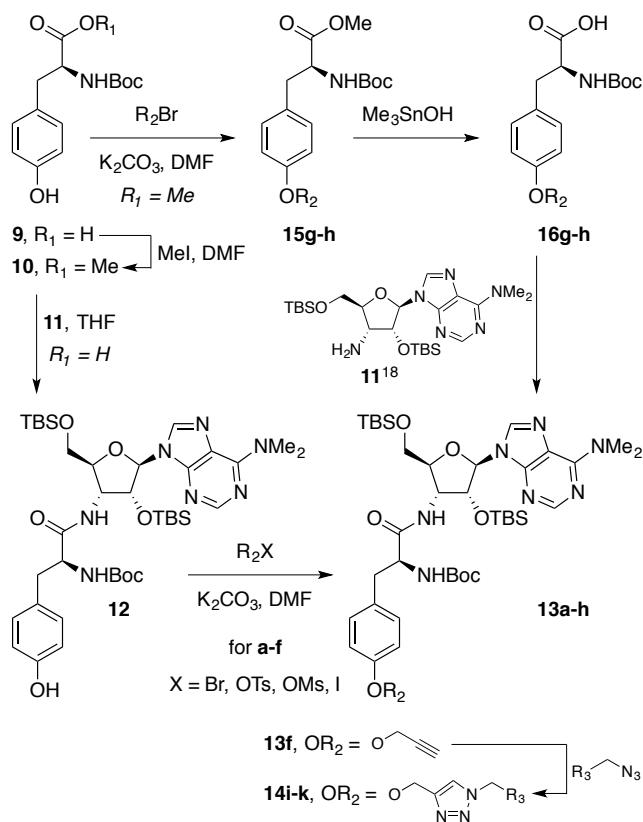


Figure 2. The structures of **6**, envisioned derivatives (**7**) and aminoacyl-tRNA (**8**).

RESULTS AND DISCUSSION

1
2
3 Syntheses of investigated derivatives **7** (Figure 2 and Table 2) were envisioned following the
4 method previously reported for phenol **12** (Scheme 1) by the Aigbirhio group.¹⁸ Starting with
5 the commercially available Boc-protected tyrosine **9**, EDC/HOBt amide coupling with TBS-
6 protected puromycin aminonucleoside **11** afforded phenol **12** which served as a common
7 intermediate to access TBS and Boc-protected derivatives of **6** (**13a-f**). These derivatives were
8 prepared from **12** by employing the classical Williamson ether synthesis²⁰ with several
9 bromides, or electrophiles containing tosylate, mesylate or iodide as leaving groups (direct
10 method). Alternatively, acid **9** was esterified to afford methyl ester **10** which was successfully
11 converted to ethers **15g-h** under analogous Williamson conditions in excellent yields (>95%).
12 Removal of the methyl ester group was performed using trimethyltin hydroxide in order to
13 avoid possible racemization at the chiral center¹⁸ and acids **16g-h** were coupled with **11** to
14 afford amides **13g-h** (Scheme 1, indirect method). Using the indirect method ether **15g** was
15 prepared in excellent yield of 95% but the additional reaction step in the synthesis of **13g**
16 negligibly lowered overall yield to 57% from 62% for the indirect and direct methods
17 respectively.
18
19
20
21
22
23
24
25
26
27
28
29
30
31
32
33
34
35
36
37
38
39
40
41
42
43
44
45
46
47
48
49
50
51
52
53
54
55
56
57
58
59
60

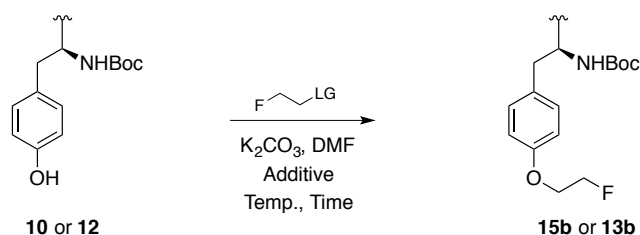


Scheme 1. Syntheses of TBS and Boc protected derivatives **7** and **14**, using direct and indirect Williamson ether methods (please refer to Supporting Information for respective yields).

Conversion to products with some electrophiles using the Williamson method was sluggish, likely because of the structural complexity of phenol **12**. In support of this theory, the reactivity of **10** and **12** with fluoroethyl electrophiles was compared (Table 1). Using mesylate as a leaving group in reaction with **12**, conversion of 16% was observed by NMR after 25 h (entry 1) due to the significant amount of by-products formed. Reaction of **12** with 2-fluoroethyl tosylate gave only trace amount of product (entry 2) whereas heating the reaction mixture to 70 °C increased the yield of **13b** to a modest 11% after 2 h and further to 44% when mixture was heated over 17 h (entries 3 and 4). On the other hand, reaction of **10** with 2-fluoroethyl tosylate proceeded with 37% NMR conversion (entry 6) at ambient temperature. Further improvement

to 42% of **15b** (entry 7) was achieved by longer reaction time at ambient temperature as well as the addition of 18-crown-6, thus avoiding the possibility of decomposition or racemization upon extended heating. The yield could be improved further to 64% by heating to reflux in MeCN (entry 8), however racemization was observed (by chiral HPLC) and therefore these reaction conditions were not pursued. To our surprise, reaction of **10** with 2-fluoroethyl mesylate showed only slightly improved conversion (vs reaction with **12**) of 20% by NMR (entry 5), for which reason we deterred from employing mesylate as the leaving group.

Table 1. Williamson ether synthesis with **10** and **12** and fluoroethyl electrophiles.

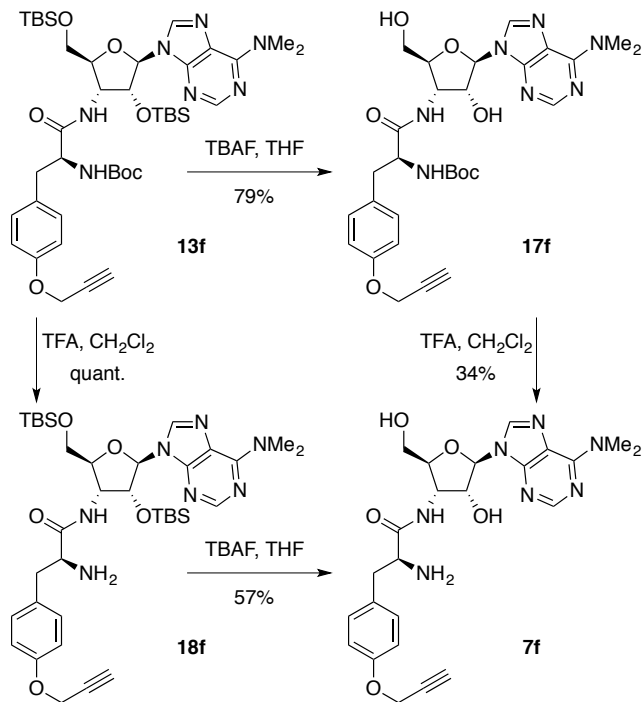


Entry	Phenol	LG	Temp. (°C)	Time (h)	Yield (%)	(S):(R)
1	12	OMs	23	25	16 ^a	—
2	12	OTs	23	19	trace	—
3	12	OTs	70	2	11	—
4	12	OTs	70	17	44	—
5	10	OMs	23	25	20 ^a	—
6	10	OTs	23	16	37 ^a	—
7	10	OTs	23	48	42 ^b	99:1
8	10	OTs	reflux	21	64 ^{b,c}	89:11

^a NMR conversion; ^b 18-c-6 used as additive; ^c MeCN was used as solvent

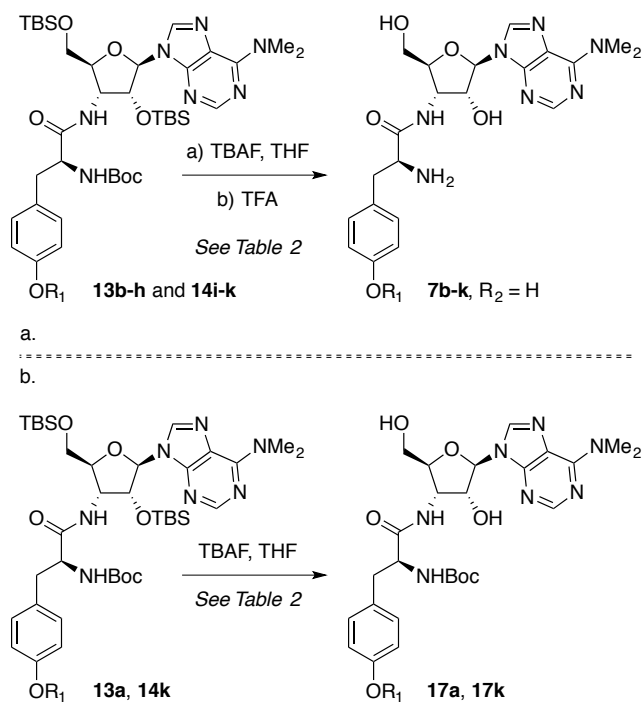
Alkyne **13f** was further reacted with aryl azides under Cu(I)-mediated [2 + 3] cycloaddition conditions to give “click” chemistry analogues **14a-c** (Scheme 1).^{16,21}

1
2
3 Structural characterization of derivative **7f** has been previously reported¹⁶ and we selected **7f**
4 as a reference to establish conditions for deprotection of both the TBS and Boc groups without
5 epimerization (Scheme 2). Alkyne **13f** was therefore treated with TBAF·THF resulting in
6 deprotection of both primary and secondary TBS groups in **17f**. TFA was employed for the
7 removal of the Boc protecting group and **7f** was afforded in 34% yield. NMR analysis of **7f** was
8 in complete agreement with that previously reported (see Supporting Information).¹⁶ An
9 alternative two step deprotection was explored in which the Boc group was removed by TFA
10 quantitatively first, and **18f** was subsequently treated with TBAF·THF to yield **7f** in 57% yield.
11 Interestingly, the primary TBS group in **13f** was cleaved during the Boc removal with TFA;
12 however it was the secondary TBS which required application of TBAF.



51
52 Scheme 2. Two step deprotection of **13f** via two routes, yielding desired **7f** in structural
53 agreement with the literature report.¹⁶
54
55
56
57
58
59
60

1
2
3 With the deprotection route established, the syntheses of other derivatives of **6** were completed
4
5
6 in a one pot two step method. Intermediates **17** and **18** were not isolated; instead the second step
7
8 was performed with the crude material to afford **7b-k** (Scheme 3a). Treatment of **13a** and **13k**
9
10 with TBAF in a single step yielded Boc-protected analogues **17a** and **17k** (Scheme 3b). Using
11
12 the synthetic method depicted in Schemes 1 and 2, derivative **7f** was obtained in 20% yield over
13
14 4 steps from commercially available starting materials, which was an improvement to the
15
16 previously reported preparation of **7f** in a total of six steps, with 9% overall yield.¹⁶ Yields
17
18 obtained for the syntheses of various derivatives of **6** are shown in Table 2.
19
20
21
22



Scheme 3. (a) Two step, one pot deprotection of TBS and Boc groups in **13/14** to afford derivatives **7**. (b) TBAF deprotection of TBS groups to obtain derivatives **17**.

Table 2. Structures of derivatives **7** and **17**, deprotection yields and inhibitory affinity data.

Entry	Derivative	OR ₁	Yield (%)	GLuc (%) ^a
1		OCH ₃	—	100
2		O-CH ₂ -CH ₂ -F	34 ^b	47
3		O-CH ₂ -C ₆ H ₄ -F	52	195
4		O-C(=O)-C ₆ H ₄ -F	14	184
5		O-CH ₂ -CH=CH ₂	38	22
6		O-CH ₂ -C≡CH	27	87
7		O-CH ₂ -CH ₂ -CH ₂ -CH ₂ -F	48	99
8		O-CH ₂ -C ₆ H ₄ -F	33	136
9		O-CH ₂ -C ₆ H ₄ -F	24	165
10		O-CH ₂ -C ₆ H ₃ (F)(CN)	15	187
11		O-CH ₂ -C ₆ H ₄ -F	37	150
12		OR ₁ = OH, R ₂ = TBS	—	112
13		OR ₁ = OCH ₃ , R ₂ = TBS	—	192
14		OR ₁ = OCH ₃ , R ₂ = H	99	156
15		OR ₁ = O-CH ₂ -C≡CH, R ₂ = H	96	184
16		OR ₁ = O-CH ₂ -C ₆ H ₄ -F, R ₂ = H	78 ^c	177

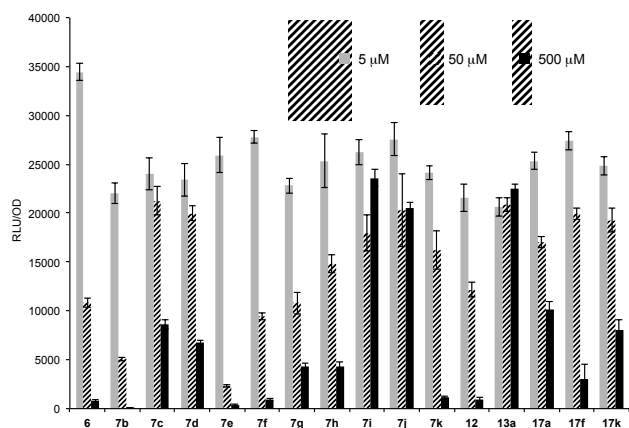
^a % GLuc production (vs. **6** inhibition) at 50 μM^b Material was accessed via two different methods;^c Material was prepared via [2 + 3] cycloaddition of azide directly with **17f**;

Please refer to Supporting information for details

1
2
3
4
5
6 With the target molecules (**6**, **7b-k**, **12**, **13a**, **17a**, **17f**, **17k**) in hand, their PS inhibitory
7
8 activity was assessed using a bioluminescent protein reporter system in bacteria. This technique
9
10 has been previously established for the assessment of compounds that inhibit PS.²² In this assay,
11
12 Gram positive bacteria *Staphylococcus aureus* 8325.4 were engineered to produce Gaussia
13
14 Luciferase (GLuc), a 19 kD photoprotein. On addition of the GLuc substrate coelenterazine, a
15
16 bioluminescent signal at 475 nm is produced proportional to the concentration of the GLuc
17
18 protein, thus providing a sensitive method with which to detect differences in PS in bacterial
19
20 culture.²³ The test compound or **6** dihydrochloride was independently applied to *S. aureus*
21
22 culture, and the quantity of GLuc protein synthesized was measured by bioluminescence after
23
24 2.5 h. Cell number was estimated by optical density (OD) to normalize the response. The
25
26 efficiency of the novel derivatives for PS inhibition compared with **6**·2HCl (set at 100%) is
27
28 displayed in Table 2.
29
30
31
32
33

34
35 Comparable PS inhibitory activity of **7f** to that of **6** was observed, as expected based on the
36
37 published data (Table 2, entries 6 and 1).¹⁶ Only three other analogues showed comparable or
38
39 better PS inhibitory effects at 50 μ M concentration: **7b**, **7e** and **7g** (entries 2, 5 and 7). At this
40
41 concentration, non-fluorinated **7e** proved the most potent PS inhibitor. Functionalization of **6**
42
43 with either aromatic substituents (entries 3, 4 and 8) or [2 + 3] cycloaddition products, the
44
45 “click” analogues (entries 9-11), resulted in reduction in inhibitory potency compared with **6**.
46
47 Similarly, masking of the hydroxyl functional groups (entries 12 and 13), in addition to amine
48
49 group (entries 14-16) confirmed importance of free hydroxyl and amine functionalities to
50
51 maintain inhibitory activity. Figure 3 shows the concentration dependence of PS inhibitory
52
53 activity of the novel derivatives. At all concentrations tested, **7b** was the most potent of the
54
55
56
57
58
59
60

1
2
3 fluorinated derivatives. At the lowest concentration tested ($5 \mu\text{M}$), **7b** reduced protein
4
5 production by 36% compared with **6**, and proved to be a superior PS inhibitor to **7e** (25%
6
7 reduction compared with **6**).
8
9
10
11
12
13

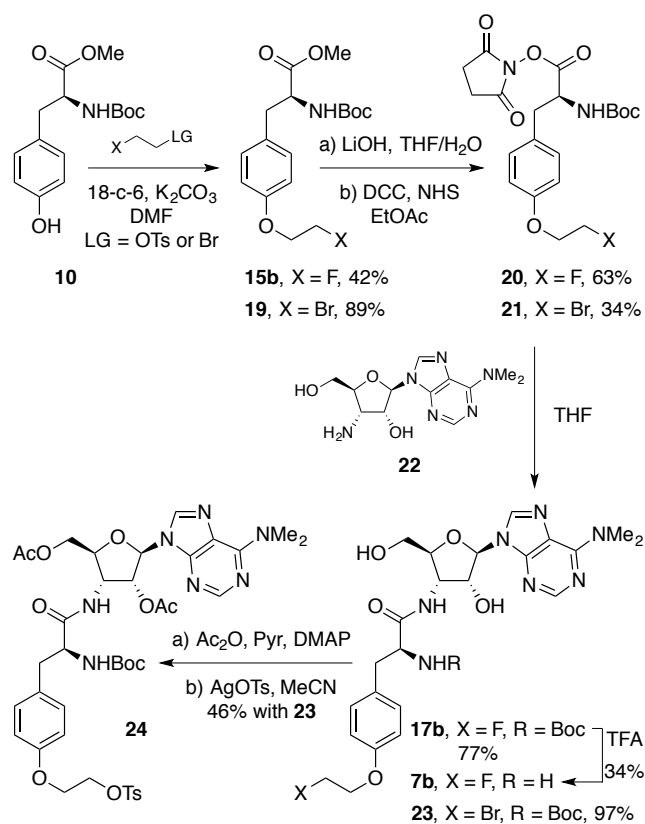


14
15
16
17
18
19
20
21
22
23
24
25
26
27
28
29
30 Figure 3. Effect of derivatives of **6** on protein synthesis, as indicated by inhibition of luciferase
31
32 synthesis. RLU/OD = relative light units/optical density.
33
34
35
36

37
38 With evidence to support the use of **7b** (FEPURO, Table 2) as the lead fluorinated compound in
39
40 the series, we next sought to develop the respective radiolabelling precursor (Scheme 4). An
41
42 obvious selection of phenol **12** (Scheme 1) as a precursor for radiosynthesis with 2-
43
44 ^{18}F fluoroethyl tosylate²⁴ was quickly discarded for following reasons: the presence of TBS
45
46 protecting groups in **12** would facilitate side reactions due to the affinity of fluoride for silicon;
47
48 and reaction of **12** with 2-fluoroethyl tosylate (Scheme 1 and Supporting Information)
49
50 proceeded with modest yield therefore predicting similarly poor conversion with 2-
51
52 ^{18}F fluoroethyl tosylate. Silicon-free protecting groups on the hydroxyl groups were necessary
53
54
55
56
57
58
59
60 for successful radiolabelling, and we chose to investigate a direct fluorination approach. The

1
2
3 radiolabelling precursor **24** (Scheme 4) was therefore envisioned as most appropriate.
4

5
6 Alongside synthesis of the radiolabelling precursor, we revisited the route to access **7b**. Methyl
7
8 ester **10** was reacted with 2-fluoroethyl tosylate to afford **15b** in 42% (Table 1), and in analogy,
9
10 reaction of **10** with 1,2-dibromoethane gave **19**, in 89% yield, using crown ether 18-c-6 as
11
12 additive. Heating this reaction to 80 °C did not induce racemization of the bromo-analogue (see
13
14 the Supporting Information). Hydrolysis of the methyl esters was accomplished with LiOH, and
15
16 using DCC the *N*-succinimidyl ester was successfully installed to yield **20** and **21**. Amide
17
18 coupling of activated esters **20** and **21** with commercially available puromycin aminonucleoside
19
20 **22** furnished 77% of **17b** and 96% of **23**. For **17b**, the Boc group was removed under acidic
21
22 conditions leading to **7b** in total of five steps and 7% overall yield. The hydroxyl groups in
23
24 bromide **23** were acetylated catalysed by DMAP, and subsequently the bromide functionality
25
26 was converted to a tosylate leaving group using silver tosylate, providing **24** in 46% yield from
27
28
29
30
31
32 **23** (Scheme 4).
33
34
35
36
37
38
39
40
41
42
43
44
45
46
47
48
49
50
51
52
53
54
55
56
57
58
59
60

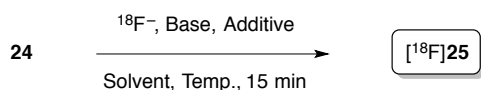


Scheme 4. Synthesis of radiolabelling precursor **24** and revisited synthesis of **7b**.

Next, conditions for radiolabelling of **24** were explored (Scheme 5) with small (288-480 MBq) amounts of $[\text{}^{18}\text{F}]\text{F}^-$ in manually conducted experiments. Aqueous $[\text{}^{18}\text{F}]\text{F}^-$ was azeotropically dried with acetonitrile in the presence of base. Variables investigated included time (5-30 min), reaction temperature (80-130 °C), reaction solvent (DMSO, MeCN, DMF), base (KHCO_3 , K_2CO_3), phase transfer agent (18-c-6, K_{222} , TBAHCO_3) and precursor quantity (5-10 mg). Full details can be found in Table 3. The optimal conversion of 22% was achieved using DMSO at 120 °C over 15 min as analysed by HPLC (entry 8). Heating the reaction to 130 °C resulted in only a slight increase in conversion to 24%, however five additional, radiolabelled species were observed by HPLC that eluted closely with $[\text{}^{18}\text{F}]\text{25}$ (entry 9). Use of

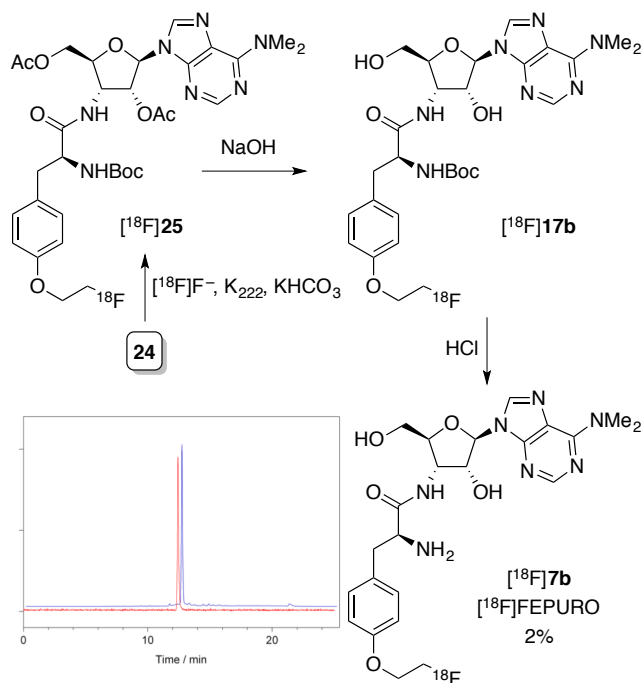
the mild base KHCO_3 with K_{222} also favoured $[^{18}\text{F}]\mathbf{25}$ formation. Reducing the amount of $\mathbf{24}$ used in the reaction resulted in a significant reduction in conversion to 12% (entry 11).

Table 3. Optimisation of radiolabelling for preparation of $[^{18}\text{F}]\mathbf{25}$ from 10 mg of $\mathbf{24}$ (0.3 mL reaction volume).



Entry	Base	Additive	Solvent	Temp. (°C)	HPLC conversion (%)
1	K_2CO_3	K_{222}	DMF	80	5
2	K_2CO_3	K_{222}	DMSO	80	13
3	K_2CO_3	K_{222}	MeCN	80	4
4	TBAHCO ₃	—	DMSO	80	12 ^a
5	KHCO_3	K_{222}	DMSO	80	18
6	KHCO_3	K_{222}	DMF	80	8
7	KHCO_3	K_{222}	DMSO	120	20 ^b
8	KHCO_3	K_{222}	DMSO	120	22
9	KHCO_3	K_{222}	DMSO	130	24 ^a
10	KHCO_3	18-c-6	DMSO	120	0
11	KHCO_3	K_{222}	DMSO	120	12 ^{a,c}

^a Formation of by-products observed; ^b 10 min reaction time; ^c 7.5 mg of $\mathbf{24}$ used



28
29
30
31
32
33
34
35

Scheme 5. Radiosynthesis of [¹⁸F]7b via nucleophilic substitution and deprotection. Overlaid radio (red) and UV (blue) HPLC traces of formulated [¹⁸F]7b, and 7b. Axes have been slightly offset for clarity.

36
37
38
39
40
41
42
43
44
45
46
47
48
49
50
51
52
53
54
55
56
57
58
59
60

After formation of [¹⁸F]25, the removal of protecting groups was investigated. Attempted total deprotection to form [¹⁸F]7b directly from [¹⁸F]25 by acidification of the DMSO reaction mixture with HCl was unsuccessful, resulting in no reaction at ambient temperature, or decomposition upon heating. For this reason a two-step method was established. In the first step, quantitative removal of both acetyl groups was accomplished in a short reaction time of 5 min using NaOH (aq.). An SPE purification was next performed to remove the DMSO from the mixture. Application of the aqueous base in the first step facilitated transfer to the SPE cartridge by solubilizing unreacted precursor **24**. The Boc-group was then removed in the second step. Successfully employed reaction conditions to form **7b** from **17b** with TFA (Scheme 4) were investigated, and although [¹⁸F]17b was completely consumed, an unidentified by-product was

1
2
3 additionally formed resulting in only 47% of [¹⁸F]**7b** by HPLC. Use of TFA was not pursued for
4
5 this reason, as well as its incompatibility with the polymer components of automated
6
7 radiochemistry modules. Instead, hydrochloric acid (3M) was successfully employed for Boc-
8
9 deprotection to form [¹⁸F]**7b** without by-products at ambient temperature over 5 min. [¹⁸F]**7b**
10
11 was purified by semi-preparative HPLC and formulated in phosphate buffered saline (PBS)
12
13 containing 10% ethanol. Structural identity of [¹⁸F]**7b** was confirmed by HPLC co-injection
14
15 with reference sample **7b** (Scheme 5).
16
17
18
19

20
21 Reactions performed using 0.9-1.8 GBq of aqueous [¹⁸F]fluoride yielded formulated [¹⁸F]**7b** in
22
23 non-decay corrected yield of 2±0.6% (n = 3) in 140 min, with specific activity of 5 GBq/μmol
24
25 and radiochemical purity of >99% after purification (Scheme 5). Conducting the radiosynthesis
26
27 manually limited any further increase in the amount of starting activity and therefore specific
28
29 activity.
30
31
32
33

34 Radiochemical stability of a formulated solution of [¹⁸F]**7b** was tested by analytical HPLC over
35
36 a three hour period, and showed no reduction in radiochemical purity.
37
38
39
40
41
42

43 CONCLUSIONS

44
45
46 We have developed a series of novel derivatives of **6**, with potential for imaging PSR by PET.
47
48 The synthesis of a common intermediate was accomplished *via* EDC/HOBt mediated amide
49
50 coupling from commercially available materials, and derivatisation of the phenol functionality
51
52 was achieved employing the classical Williamson synthesis in good yields. Using a luciferase
53
54 PS assay **7b** was identified as the lead compound having higher PSR inhibitory potency than
55
56
57
58
59
60

reference **6**. The radiolabelling precursor **24** was prepared in seven steps with 14% overall yield and successfully employed in the radiosynthesis of [¹⁸F]**7b** via nucleophilic substitution.

Radiolabelled [¹⁸F]**7b** was prepared in excellent radiochemical purity. Implementation of a modular radiosynthesis of [¹⁸F]**7b** as well as *in vitro* and *in vivo* evaluation of [¹⁸F]**7b** are currently underway in our laboratories and will be reported in a due course.

EXPERIMENTAL SECTION

General. All reactions requiring anhydrous conditions were conducted in oven-dried glass apparatus under an atmosphere of inert gas. All reagents were purchased from Sigma-Aldrich or Alfa Aesar and used without further purification, unless otherwise stated. Preparative chromatographic separations were performed on Aldrich Science silica gel 60 (35-75 μm) and reactions followed by TLC analysis using Sigma-Aldrich silica gel 60 plates (2-25 μm) with fluorescent indicator (254 nm) and visualized with UV or potassium permanganate. ¹H and ¹³C NMR spectra were recorded in Fourier transform mode at the field strength specified on a Bruker Avance 400 MHz or a Bruker Avance 300 MHz spectrometer. Spectra were obtained in the specified deuterated solvents in 5 mm diameter tubes. Chemical shift in ppm is quoted relative to residual solvent signals calibrated as follows: **CDCl₃** δ_H (*CHCl₃*) = 7.26 ppm, δ_C = 77.2 ppm; **(CD₃)₂SO** δ_H (*CD₃SOCHD₂*) = 2.50 ppm, δ_C = 39.5 ppm; **MeOD-*d*₄** δ_H (*CD₂HOD*) = 3.31 ppm, δ_C = 49.0 ppm; **(CD₃)₂NC(O)**D**** δ_H (*((CD₃)₂NC(O)H*) = 7.92 ppm, δ_C = 165.5 ppm. Multiplicities in the ¹H NMR spectra are described as: s = singlet, d = doublet, t = triplet, q = quartet, quint. = quintet, m = multiplet, b = broad; coupling constants are reported in Hz. Numbers in parentheses following carbon atom chemical shifts refer to the number of attached

1
2
3 hydrogen atoms as revealed by the DEPT/HSQC spectral editing technique. Mass spectra were
4
5 recorded on a Waters Micromass LCT instrument, a Bruker MicroTOF mass spectrometer using
6
7 electrospray Ionisation (ESI), or by the EPSRC Mass Spectrometry Service at the University of
8
9 Swansea. Purity of compounds was $\geq 95\%$ as determined by analytical LC on a Waters Acquity-
10
11 H UPLC or Agilent Series 1200 system with UV detection ($\lambda = 254$ nm). The general
12
13 UPLC/HPLC methods were as follows. Waters general method: 0-4 min, 5-95% aq. MeCN at
14
15 0.6 mL/min (column: BEH C18, 1.7 μm , 2.1x50 mm. Agilent general method: 0- 1 min 5% B;
16
17 1-15 min 5-95% B; 15-18 min 95% B; 18-20 min 95-5% B; 20-25 min 5% B. A flow rate of 1
18
19 mL/min was used. Unless otherwise stated, solvent A = H₂O and B = MeCN. A Phenomenex
20
21 Luna C18(2) column (150 mm x 4.6 mm) was used. All radioactive manipulations were
22
23 performed in designated lead shielded hot cells to reduce operator dose. [¹⁸F]Fluoride was
24
25 purchased from PETNET Nottingham, and was supplied as [¹⁸F]fluoride in H₂[¹⁸O]O. Seppak
26
27 tC18 light cartridges were purchased from Waters. Radiochemical incorporation was
28
29 determined by the percentage of the desired product from integration of the analytical HPLC
30
31 radiotracer. Where radiochemical yields are given, they are calculated from HPLC purified
32
33 material as a percentage of starting aqueous [¹⁸F]fluoride, and are not corrected for decay. Semi-
34
35 preparative HPLC was performed using a Knauer Smartline pump, equipped with Knauer Azura
36
37 UV detector (254 nm) and diode radiodetector (Carroll Ramsey, USA), and a custom built
38
39 apparatus for HPLC loop load and product collection. Data were collected using SingleStream
40
41 software (Dr. R. Fortt). A Phenomenex Synergi Hydro-RP column (250 x 10 mm) 4 μ 80A with
42
43 guard was used, with an isocratic method. The eluant was composed of 30% MeCN in 70%
44
45 ammonium acetate (aq. 50 mM), with a flow rate of 2 mL/min.
46
47
48
49
50
51
52
53
54
55
56
57
58
59
60

1
2
3
4
5
6
7
8
9
10
11
12
13
14
15
16
17
18
19
20
21
22
23
24
25
26
27
28
29
30
31
32
33
34
35
36
37
38
39
40
41
42
43
44
45
46
47
48
49
50
51
52
53
54
55
56
57
58
59
60

(S)-2-Amino-N-{(2S,3S,4R,5R)-5-[6-(dimethylamino)-9H-purin-9-yl]-4-hydroxy-2-(hydroxymethyl)tetrahydrofuran-3-yl}-3-[4-(2-fluoroethoxy)phenyl]propanamide (7b).

17b (40.1 mg, 0.07 mmol) was dissolved in TFA (0.5 mL). The reaction stirred at room temperature for 10 min, after which the volatiles were removed under a stream of N₂. The resulting solid was rinsed with diethyl ether (2x1 mL) and dried under a stream of N₂. The solid was redissolved in EtOAc (15 mL), and extracted into H₂O (15 mL). The aqueous layer was retained, and saturated aq. NaHCO₃ (10 mL) was added. The product was extracted into EtOAc (2x10 mL), and washed with H₂O (10 mL). The organic layer was dried (MgSO₄), and evaporated under reduced pressure. The product was purified by column chromatography on silica (eluting with 5% MeOH/CH₂Cl₂ containing 1% NEt₃) yielding a white solid (11.4 mg, 0.02 mmol, 34%): ¹H NMR (400 MHz, DMSO-*d*₆) δ 8.44 (s, 1H), 8.23 (s, 1H), 8.08 (bs, 1H), 7.16 (d, *J* = 8.6 Hz, 2H), 6.88 (d, *J* = 8.6 Hz, 2H), 6.13 (bd, *J* = 2.9 Hz, 1H), 5.98 (d, *J* = 2.7 Hz, 1H), 5.15 (bt, *J* = 5.2 Hz, 1H), 4.80-4.64 (dm, *J*_{F-C-H} = 47.8 Hz, 2H), 4.51-4.42 (m, 2H), 4.25-4.13 (dm, *J*_{F-C-H} = 30.2 Hz, 2H), 3.96-3.90 (bm, 1H), 3.72-3.65 (b m, 1H) 3.54- 3.26 (b m, 8H), 2.92 (dd, *J* = 13.5, 5.0 Hz, 1H), 2.57 (dd, *J* = 13.5, 8.5 Hz, 1H) ppm; ¹³C NMR (100 MHz, DMSO-*d*₆) δ 174.3 (0), 156.6 (0), 154.2 (0), 151.7 (1), 149.5 (0), 137.8 (1), 130.7 (0), 130.2 (1, 2C), 119.5 (0), 114.1 (1, 2C), 89.3 (1), 83.5 (1), 82.1 (2, d, *J* = 166.6 Hz), 73.1 (1), 66.9 (2, d, *J* = 19.0 Hz), 60.9 (2), 56.0 (1), 50.0 (1), 39.7 (2, obscured by solvent, visible by DEPT-135), 37.7 (b, 3, 2C) ppm; ¹⁹F NMR (376 MHz, DMSO-*d*₆) δ -224.7 (tt, *J*_{H-C-F} = 47.8, *J*_{H-C-F} = 30.2 Hz) ppm; HRMS *m/z* [M + H]⁺ 504.2372 (calcd. 504.2365 for C₂₃H₃₁FN₇O₅⁺); HPLC (Solvent A = ammonium acetate, 50 mM, solvent B = MeOH) *R*_t = 12.2 min.

(S)-2-amino-N-{(2S,3S,4R,5R)-5-[6-(dimethylamino)-9H-purin-9-yl]-4-hydroxy-2-(hydroxymethyl)tetrahydrofuran-3-yl}-3-[4-[2-(¹⁸F)fluoro]ethoxy]phenyl}propanamide

1
2
3 ([¹⁸F]7b). The optimized procedure was as follows: aqueous [¹⁸F]fluoride (0.9-1.8 GBq) was
4 added to a mixture of K₂₂₂ (5.0 mg) and KHCO₃ (50 μL, 0.1 M) in MeCN (0.5 mL) in a v-vial
5 equipped with stirring bar. The mixture was dried azeotropically at 110 °C under a stream of N₂
6 (without stirring). Two further portions of MeCN (2x0.5 mL) were added to ensure complete
7 drying (total drying time ca. 30 min). Precursor **24** (10.0 mg), was dissolved in DMSO (0.3 mL,
8 anhydrous) and added to the dried [¹⁸F]fluoride. The reaction was heated to 120 °C for 15 min
9 with stirring. After cooling to room temperature, NaOH (1 M, 3 mL) was added and stirred for
10 5 min, followed by DMSO (0.7 mL). The reaction mixture was loaded to a pre-conditioned
11 (MeCN 2 mL; H₂O 5 mL) 'C18 Seppak light cartridge, and the cartridge was washed with H₂O
12 (4 mL). The cartridge was briefly dried for 2 min after washing. The cartridge was eluted with
13 MeCN (0.5 mL), concentrated under a stream of N₂ at 80 °C for 5 min, cooled, and HCl (3 M,
14 300 μL) added. The reaction stirred for 5 min at room temperature. After neutralization with
15 NaOH (1M) and dilution with mobile phase (1 mL), the mixture was loaded to a semi-
16 preparative HPLC system for purification. The radioactive peak corresponding to the product
17 (*R_t* = 12 min) was collected. The HPLC cut was diluted with H₂O (15 mL), loaded to a primed
18 'C18 light cartridge (EtOH 2mL; H₂O 5 mL), and washed with H₂O (2 mL). The desired product
19 [¹⁸F]7b was eluted with EtOH (300 μL) and diluted in phosphate buffered saline (2.7 mL).
20 Product [¹⁸F]7b was isolated in non-decay corrected yield of 2±0.6% (n = 3), with specific
21 activity of 5 GBq/μmol and radiochemical purity of >99%.

22
23
24
25
26
27
28
29
30
31
32
33
34
35
36
37
38
39
40
41
42
43
44
45
46
47
48
49 **Methyl-(S)-2-[(*tert*-butoxycarbonyl)amino]-3-[4-(2-fluoroethoxy)phenyl]propanoate**

50 (**BocTyr(EtF)OMe, 15b**). Boc(L)TyrOMe (1.01 g, 3.4 mmol, 1eq) was dissolved in DMF (6
51 mL) and K₂CO₃ (3.23 g, 23.4 mmol, 6.9 eq) was added. 18-Crown-6 (0.10 g, 0.4 mmol, 0.1 eq)
52 and 2-fluoroethyl tosylate (0.82 g, 3.8 mmol, 1.1 eq) were added and the reaction stirred at
53
54
55
56
57
58
59
60

1
2
3 room temperature for 48 h. H₂O (25 mL) was added to the reaction, and the product extracted
4 into EtOAc (2x30 mL). The combined organics were washed with brine (2x30 mL), dried
5 (MgSO₄), and evaporated under reduced pressure. The product was purified by silica
6 chromatography (eluting with 20% EtOAc/hexane) yielding a colorless oil, which solidified on
7 standing (0.49 g, 1.4 mmol, 42%): ¹H NMR (400 MHz, CDCl₃) δ 7.07 (d, *J* = 8.6 Hz, 2H), 6.88
8 (d, *J* = 8.6 Hz, 2H), 4.97 (d, *J* = 7.9 Hz, 1H), 4.77 (dt, *J* = 47.4, 4.2 Hz, 2H), 4.57 (m, 1H), 4.22
9 (dt, *J* = 27.7, 4.2 Hz, 2H), 3.73 (s, 3H), 3.09-2.96 (m, 2H), 1.44 (s, 9H) ppm; HRMS *m/z* [M +
10 Na]⁺ 364.1542 (calcd. 364.1531 for C₁₇H₂₄FNNaO₅⁺); HPLC *R*_t = 13.3 min. The spectral data
11 were in complete agreement with the literature reported values.²⁵

12
13
14
15
16
17
18
19
20
21
22
23
24
25
26 ***Tert*-butyl [(*S*)-1-((2*S*,3*S*,4*R*,5*R*)-5-[6-(dimethylamino)-9*H*-purin-9-yl]-4-hydroxy-2-**
27 **(hydroxymethyl)tetrahydrofuran-3-yl]amino)-3-[4-(2-fluoroethoxy)phenyl]-1-oxopropan-**
28 **2-yl]carbamate (17b)**. Puromycin aminonucleoside (0.14 g, 0.5 mmol, 1 eq) was dissolved in
29 THF (8 mL) and BocTyr(EtF)OSu **20** (0.20 g, 0.5 mmol, 1 eq) was added. The reaction stirred
30 at room temperature for 20 h. The reaction was diluted with H₂O and product extracted with
31 EtOAc (3x20 mL). The organic extracts were washed with H₂O (20 mL) and brine (20 mL),
32 dried (MgSO₄), and evaporated to dryness. The product was purified by column
33 chromatography on silica (eluting with 5% MeOH/CH₂Cl₂) yielding a white solid (0.22 g, 3.6
34 mmol, 77%): ¹H NMR (400 MHz, DMSO-*d*₆) δ 8.44 (s, 1H), 8.24 (s, 1H), 8.00 (d, *J* = 7.6 Hz,
35 1H), 7.20 (d, *J* = 8.5 Hz, 2H), 6.90-6.84 (m, 3H), 6.06 (d, *J* = 4.7 Hz, 1H), 5.99 (d, *J* = 2.8 Hz,
36 1H), 5.16 (bm, 1H), 4.72 (m, *J*_{H-C-F} = 47.8 Hz, 2H), 4.53-4.43 (m, 2H), 4.24-4.13 (m, *J*_{H-C-C-F} =
37 30.2 Hz, 3H), 3.96-3.91 (bm, 1H), 3.68 (bd, *J* = 11.6 Hz, 1H), 3.61-3.34 (bm, 7H), 2.91 (dd, *J*
38 = 13.6, 4.6 Hz, 1H), 2.70 (dd, *J* = 13.3, 9.9 Hz, 1H), 1.30 (s, 9H) ppm; ¹³C NMR (100 MHz,
39 DMSO-*d*₆) δ 172.0 (0), 156.6 (0), 155.1 (0), 154.2 (0), 151.8 (1), 149.6 (0), 137.8 (1), 130.2 (1,
40
41
42
43
44
45
46
47
48
49
50
51
52
53
54
55
56
57
58
59
60

2C), 119.5 (0), 114.0 (1, 2C), 89.2 (1), 83.3 (1), 82.1 (2) (d, $J = 166.5$ Hz), 78.0 (0), 73.0 (1), 66.9 (2, d, $J = 19.0$ Hz), 60.8 (2), 55.8 (1), 50.2 (1), 37.8 (3, 2C), 36.8 (2), 28.0 (3, 3C) ppm.

One carbon resonance was missing (quaternary aromatic carbon); ^{19}F NMR (376 MHz, DMSO- d_6) δ -224.7 (tt, $J_{\text{H-C-F}} = 47.8$, $J_{\text{H-C-C-F}} = 30.2$ Hz) ppm; HRMS $[\text{M} + \text{H}]^+$ m/z 604.2887 (calcd. 604.2890 for $\text{C}_{28}\text{H}_{39}\text{FN}_7\text{O}_7^+$); HPLC $R_t = 10.9$ min.

(S)-2-[(Tert-butoxycarbonyl)amino]-3-[4-(2-fluoroethoxy)phenyl]propanoic acid

(BocTyr(EtF)OH, *en route to 20*). BocTyr(EtF)OMe **15b** (0.46 g, 1.4 mmol) was dissolved in THF (8 mL) and cooled to 0 °C in an ice bath. LiOH (aq. 2M, 2 mL) was added and the reaction stirred for 2 h. The THF was evaporated and the mixture acidified with KHSO_4 (5%, 30 mL).

The product was extracted into EtOAc (2x30 mL), and the combined organic extracts were dried (MgSO_4), filtered and evaporated to dryness. The product was isolated as a white solid (0.42 g, 1.3 mmol, 93%). No further purification was necessary. ^1H NMR (400 MHz, CDCl_3) δ 7.11 (d, $J = 8.6$ Hz, 2H), 6.87 (d, $J = 8.6$ Hz, 2H), 4.92 (d, $J = 7.3$ Hz, 1H), 4.74 (dt, $J = 47.4$, 4.2 Hz, 2H), 4.57 (m, 1H), 4.19 (dt, $J = 27.8$, 4.2 Hz, 1H), 3.17-3.00 (m, 2H), 1.42 (s, 9H) ppm; ^{13}C NMR (100 MHz, CDCl_3) δ 176.5 (0), 157.8 (0), 155.6 (0), 130.7 (1, 2C), 128.6 (0), 115.0 (1, 2C), 82.1 (2, d, $J = 170.6$ Hz), 80.5 (0), 67.3 (2, d, $J = 20.5$ Hz), 54.6 (1), 37.1 (2), 28.5 (3, 3C) ppm; ^{19}F NMR (376 MHz, CDCl_3) δ -224.9 (tt, $J_{\text{H-C-F}} = 47.4$, $J_{\text{H-C-C-F}} = 27.8$ Hz) ppm; HRMS m/z $[\text{M} - \text{H}]^-$ 326.1408 (calcd. 326.1409 for $\text{C}_{16}\text{H}_{21}\text{FNO}_5^-$); HPLC (Solvent A = $\text{H}_2\text{O} + 0.1\%$ TFA; B = MeCN + 0.1% TFA) $R_t = 11.7$ min.

2,5-Dioxopyrrolidin-1-yl (S)-2-[(tert-butoxycarbonyl)amino]-3-[4-(2-

fluoroethoxy)phenyl]propanoate (BocTyr(EtF)OSu, **20**). BocTyr(EtF)OH (0.41 g, 1.3 mmol, 1 eq), was dissolved in EtOAc (10 mL) and *N*-hydroxysuccinimide (0.15 g, 1.3 mmol, 1 eq) was

1
2
3 added. The mixture was cooled to 0 °C in an ice bath. Dicyclohexylcarbodiimide (0.26 g, 1.3
4
5 mmol, 1 eq) was added dropwise as a solution in EtOAc (10 mL). The reaction stirred at room
6
7 temperature for 16 h, after which the white precipitate was filtered off. The filtrate was
8
9 evaporated to dryness, then recrystallized from hot 2-propanol. The resulting solid was filtered
10
11 and dried *in vacuo* (0.36 g, 0.8 mmol, 68%): ¹H NMR (400 MHz, CDCl₃) δ 7.21 (d, *J* = 8.6 Hz,
12
13 2H), 6.88 (d, *J* = 8.6 Hz, 2H), 4.95-4.83 (m, 1H), 4.74 (dt, *J* = 47.4, 4.2 Hz, 2H), 4.20 (dt, *J* =
14
15 27.7, 4.2 Hz, 2H), 3.28-3.07 (m, 2H), 2.86 (s, 4H), 1.42 (s, 9H) ppm; ¹³C NMR (100 MHz,
16
17 CDCl₃) δ 168.8 (0), 167.9 (0), 157.9 (0), 154.8 (0), 131.0 (1, 2C), 127.4 (0), 115.0 (1, 2C), 82.1
18
19 (2, d, *J* = 170.6 Hz), 80.7 (0), 67.3 (2, d, *J* = 20.6 Hz) 52.9 (1), 37.5 (2), 28.4 (3, 3C), 25.8 (2,
20
21 2C) ppm; ¹⁹F NMR (376 MHz, CDCl₃) δ -224.9 (tt, *J*_{H-C-F} = 47.4, *J*_{H-C-C-F} = 27.7 Hz) ppm;
22
23 HRMS [M + Na]⁺ *m/z* 447.1530 (calcd. 447.1538 for C₂₀H₂₅FN₂NaO₇⁺); HPLC:
24
25 BocTyr(EtF)OSu appeared to decompose on HPLC analysis under all conditions tested, using
26
27 both normal and reverse phase columns.
28
29
30
31
32
33

34
35 ***In vitro* assays.** *S. aureus* 8325.4 (pUNKP_{xyt/tet}::GLuc) was grown overnight in 5 mL tryptone
36
37 soya broth (TSB), with erythromycin (5 μg/mL) and lincomycin (25 μg/mL) at 37 °C with 250
38
39 rpm shaking. The overnight culture was diluted to an optical density (OD₆₀₀) of 0.05 with fresh
40
41 TSB, and anhydrotetracycline (ATc, 40 ng/mL) was added to induce GLuc expression.
42
43 Compounds for assessment were prepared as stock solutions of 50 mM in DMSO, and diluted
44
45 to final concentrations of 5 μM, 50 μM and 500 μM, containing 1% DMSO. To a 96-well plate
46
47 (Corning, black, clear bottom) was added bacterial culture (180 μL) and test compound (20 μL),
48
49 control wells contained 1% DMSO; all experiments were performed in triplicate. *Bacterial cell*
50
51 *number*: Plates were incubated at 37 °C in a 96 well plate reader (Tecan), and optical density
52
53 (OD₆₀₀) was recorded every 15 min for 2.5 h. *Bioluminescence*: After 2.5 h, and whilst in the
54
55
56
57
58
59
60

1
2
3 Tecan plate reader, coelenterazine (20 μM , 50 μL) was added to each well and bioluminescence
4
5 immediately recorded. The bioluminescent signal was normalized with optical density to correct
6
7 for cell number and reported in relative light units per OD (RLU/OD). Error bars indicate
8
9 standard deviation from the mean.
10
11
12
13
14
15
16

17 ASSOCIATED CONTENT

20 **Supporting Information.**

21
22
23 Full experimental details for the synthesis of analogues of **6**, NMR spectral data, radio-HPLC
24
25 traces and stability study data are available in the Supporting Information. This material is
26
27 available free of charge via the Internet at <http://pubs.acs.org>.
28
29
30
31

32 AUTHOR INFORMATION

33 **Corresponding Authors**

34
35
36
37 * Email: helen.betts@nottingham.ac.uk. Tel: 0044 (0)115 9709172; sms96@cam.ac.uk Tel:
38
39 0044 (0)1223 748188.
40
41
42

43 **Author Contributions**

44
45
46 ‡These authors contributed equally. All authors have given approval to the final version of the
47
48 manuscript.
49
50

51 **Funding Sources**

52
53
54 H.M.B. acknowledges the Royal Society of Chemistry Research Fund for partial funding of this
55
56 project, and the NIHR Clinical Research Network (East Midlands) for funding her post. We are
57
58
59
60

1
2
3 grateful to the UK Medical Research Council (MRC) for funding (Grant number G9219778).
4
5 Carmen Tong was supported by the MRC/University of Nottingham Doctoral Training
6
7 Program. SMS acknowledges EPSRC Mass Spectrometry Facility for funding her attendance at
8
9 the Mass Spectrometry Summer School 2016.
10
11

12 13 Notes

14
15
16 The authors declare no competing financial interests.
17
18

19 20 ACKNOWLEDGMENT

21
22 Dr. W. Chan (University of Nottingham) is acknowledged for access to synthetic chemistry
23
24 facilities. The EPSRC Mass Spectrometry Facility at the University of Swansea is
25
26 acknowledged for performing HRMS analyses.
27
28

29 30 ABBREVIATIONS

31
32 DSC disuccinimidyl; EDC, 1-ethyl-3-(3-dimethylaminopropyl)carbodiimide; [¹⁸F]FET, *O*-(2-
33
34 [¹⁸F]fluoroethyl) tyrosine; [¹⁸F]FPHCYS, *S*-(3-[¹⁸F]fluoropropyl)homocysteine; [¹⁸F]FTYR, 2-
35
36 [¹⁸F]fluorotyrosine; HOBt, hydroxybenzotriazole; [¹¹C]LEU, carbon-11 leucine; [¹¹C]MET,
37
38 carbon-11 methionine; PET, positron emission tomography; PURO, puromycin; SPE, solid
39
40 phase extraction; TBS, *tert*-butyldimethylsilyl.
41
42
43
44

45 46 REFERENCES

- 47
48 (1) Sonenberg, N.; Hinnebusch, A. G. Regulation of Translation Initiation in Eukaryotes:
49
50 Mechanisms and Biological Targets. *Cell* **2009**, *136*, 731–745.
51
52
53 (2) Bhat, M.; Robichaud, N.; Hulea, L.; Sonenberg, N.; Pelletier, J.; Topisirovic, I. Targeting
54
55 the Translation Machinery in Cancer. *Nat. Rev. Drug Discovery* **2015**, *14*, 261–278.
56
57
58
59
60

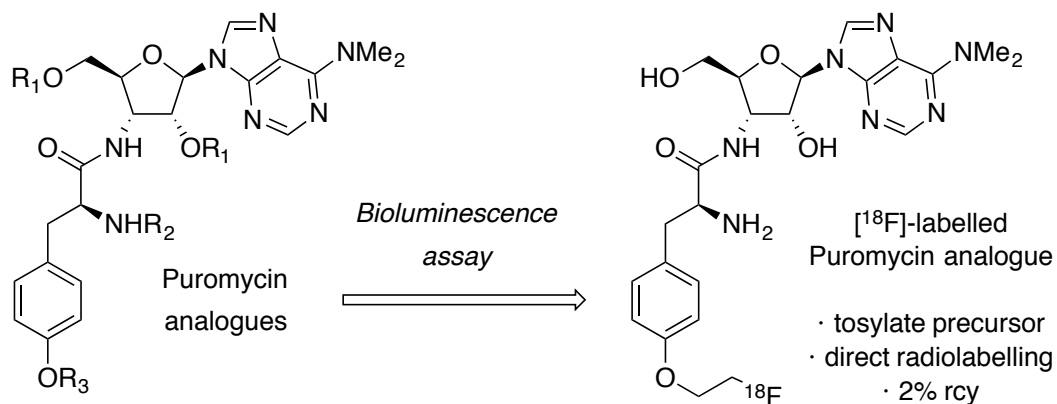
- 1
2
3
4
5
6
7
8
9
10
11
12
13
14
15
16
17
18
19
20
21
22
23
24
25
26
27
28
29
30
31
32
33
34
35
36
37
38
39
40
41
42
43
44
45
46
47
48
49
50
51
52
53
54
55
56
57
58
59
60
- (3) Halliday, M.; Mallucci, G. R. Review: Modulating the Unfolded Protein Response to Prevent Neurodegeneration and Enhance Memory. *Neuropathol. Appl. Neurobiol.* **2015**, *41*, 414–427.
- (4) Miller, P. W.; Long, N. J.; Vilar, R.; Gee, A. D. Synthesis of ¹¹C, ¹⁸F, ¹⁵O, and ¹³N Radiolabels for Positron Emission Tomography. *Angew. Chem. Int. Ed. Engl.* **2008**, *47*, 8998–9033.
- (5) Hawkins, R. A.; Huang, S. C.; Barrio, J. R.; Keen, R. E.; Feng, D.; Mazziotta, J. C.; Phelps, M. E. Estimation of Local Cerebral Protein Synthesis Rates with L-[1-¹¹C]leucine and PET: Methods, Model, and Results in Animals and Humans. *J. Cereb. Blood Flow Metab.* **1989**, *9*, 446–460.
- (6) Ishiwata, K.; Vaalburg, W.; Elsinga, P. H.; Paans, a M.; Woldring, M. G. Comparison of L-[1-¹¹C]methionine and L-Methyl-[¹¹C]methionine for Measuring in Vivo Protein Synthesis Rates with PET. *J. Nucl. Med.* **1988**, *29*, 1419–1427.
- (7) Bourdier, T.; Shepherd, R.; Berghofer, P.; Jackson, T.; Fookes, C. J. R.; Denoyer, D.; Dorow, D. S.; Greguric, I.; Gregoire, M.-C.; Hicks, R. J.; Katsifis, A. Radiosynthesis and Biological Evaluation of L- and D-S-(3-[¹⁸F]fluoropropyl)homocysteine for Tumor Imaging Using Positron Emission Tomography. *J. Med. Chem.* **2011**, *54*, 1860–1870.
- (8) Laverman, P.; Boerman, O. C.; Corstens, F. H. M.; Oyen, W. J. G. Fluorinated Amino Acids for Tumour Imaging with Positron Emission Tomography. *Eur. J. Nucl. Med. Mol. Imaging* **2002**, *29*, 681–690.
- (9) Nathans, D. Puromycin Inhibition of Protein Synthesis: Incorporation of Puromycin Into

- 1
2
3 Peptide Chains. *Proc. Natl. Acad. Sci. U. S. A.* **1964**, *51*, 585–592.
4
5
6
7 (10) Yarmolinsky, M. B.; Haba, G. L. Inhibition By Puromycin of Amino Acid Incorporation
8
9 Into Protein. *Proc. Natl. Acad. Sci. U. S. A.* **1959**, *45*, 1721–1729.
10
11
12 (11) Eigner, S.; Vera, D. R. B.; Fellner, M.; Loktionova, N. S.; Piel, M.; Lebeda, O.; Rösch, F.;
13
14 Roß, T. L.; Henke, K. E. Imaging of Protein Synthesis: In Vitro and in Vivo Evaluation of
15
16 (44)Sc-DOTA-Puromycin. *Mol. Imaging Biol.* **2013**, *15*, 79–86.
17
18
19
20 (12) Miyamoto-Sato, E.; Nemoto, N.; Kobayashi, K.; Yanagawa, H. Specific Bonding of
21
22 Puromycin to Full-Length Protein at the C-Terminus. *Nucleic Acids Res.* **2000**, *28*, 1176–
23
24 1182.
25
26
27
28 (13) Starck, S. R.; Qi, X.; Olsen, B. N.; Roberts, R. W. The Puromycin Route to Assess Stereo-
29
30 and Regiochemical Constraints on Peptide Bond Formation in Eukaryotic Ribosomes. *J.*
31
32 *Am. Chem. Soc.* **2003**, *125*, 8090–8091.
33
34
35
36 (14) Starck, S. R.; Roberts, R. W. Puromycin Oligonucleotides Reveal Steric Restrictions for
37
38 Ribosome Entry and Multiple Modes of Translation Inhibition. *RNA* **2002**, *8*, 890–903.
39
40
41
42 (15) Schmidt, E. K.; Clavarino, G.; Ceppi, M.; Pierre, P. SUnSET, a Nonradioactive Method to
43
44 Monitor Protein Synthesis. *Nat. Methods* **2009**, *6*, 275–277.
45
46
47 (16) Liu, J.; Xu, Y.; Stoleru, D.; Salic, A. Imaging Protein Synthesis in Cells and Tissues with
48
49 an Alkyne Analog of Puromycin. *Proc. Natl. Acad. Sci. U. S. A.* **2012**, *109*, 413–418.
50
51
52
53 (17) Eigner, S.; Beckford Vera, D. R.; Fellner, M.; Loktionova, N. S.; Piel, M.; Melichar, F.;
54
55 Rösch, F.; Roß, T. L.; Lebeda, O.; Henke, K. E. Measurement of Protein Synthesis: In
56
57
58
59
60

- 1
2
3 Vitro Comparison of (68)Ga-DOTA-Puromycin, [(3)H]tyrosine, and 2-Fluoro-
4 [(3)H]tyrosine. *Recent Results Cancer Res.* **2013**, *194*, 269–283.
5
6
7
8
9 (18) Sephton, S. M.; Aigbirhio, F. I. Synthesis and Radiosynthesis of Carbon-11 Labelled
10 Puromycin as a Potential PET Candidate for Imaging Protein Synthesis In Vivo. *ACS*
11 *Med. Chem. Lett.* **2016**, *7*, 647–651.
12
13
14
15
16
17 (19) Nathans, D.; Neidle, A. Structural Requirements for Puromycin Inhibition of Protein
18 Synthesis. *Nature* **1963**, *197*, 1076–1077.
19
20
21
22
23 (20) Blakemore, P.; Milicevic, S.; Perera, H.; Shvarev, A.; Zakharov, L. Determination of P K
24 a Values for Diether Derivatives of 7,7'-Dihydroxy-8,8'-Biquinolyl: Dependence of
25 Basicity on Interannular Dihedral Angle. *Synthesis (Stuttg.)*. **2008**, 2271–2277.
26
27
28
29
30 (21) Glaser, M.; Arstad, E. “Click Labeling” with 2-[18F]fluoroethylazide for Positron
31 Emission Tomography. *Bioconjugate Chem.* **2007**, *18*, 989–993.
32
33
34
35
36 (22) Lampinen, J.; Virta, M.; Karp, M. Use of Controlled Luciferase Expression To Monitor
37 Chemicals Affecting Protein Synthesis. *Appl. Environ. Microbiol.* **1995**, *61*, 2981–2989.
38
39
40
41
42 (23) Tong, C.; Chan, W.; Williams, P.; Hill, P. Screening for Inhibitors of Staphylococcal
43 Sortase A as Novel Anti-Infective Agents Using a Gaussia Luciferase Cell Based Reporter
44 Assay. *19th International Symposium on Bioluminescence and Chemiluminescence* May
45 29 - June 2, 2016, Tsukuba, Japan, A1-6.
46
47
48
49
50
51
52 (24) Kniess, T.; Laube, M.; Brust, P.; Steinbach, J. 2-[18 F]Fluoroethyl Tosylate – a Versatile
53 Tool for Building 18 F-Based Radiotracers for Positron Emission Tomography. *Med.*
54 *Chem. Commun.* **2015**, *6*, 1714–1754.
55
56
57
58
59
60

- 1
2
3
4
5
6
7
8
9
10
11
12
13
14
15
16
17
18
19
20
21
22
23
24
25
26
27
28
29
30
31
32
33
34
35
36
37
38
39
40
41
42
43
44
45
46
47
48
49
50
51
52
53
54
55
56
57
58
59
60
- (25) Paramanik, M.; Singh, R.; Mukhopadhyay, S.; Ghosh, S. K. Catalytic Nucleophilic Fluorination by an Imidazolium Ionic Liquid Possessing Trialkylphosphine Oxide Functionality. *J. Fluorine Chem.* **2015**, *178*, 47–55.

Table of Contents Graphic



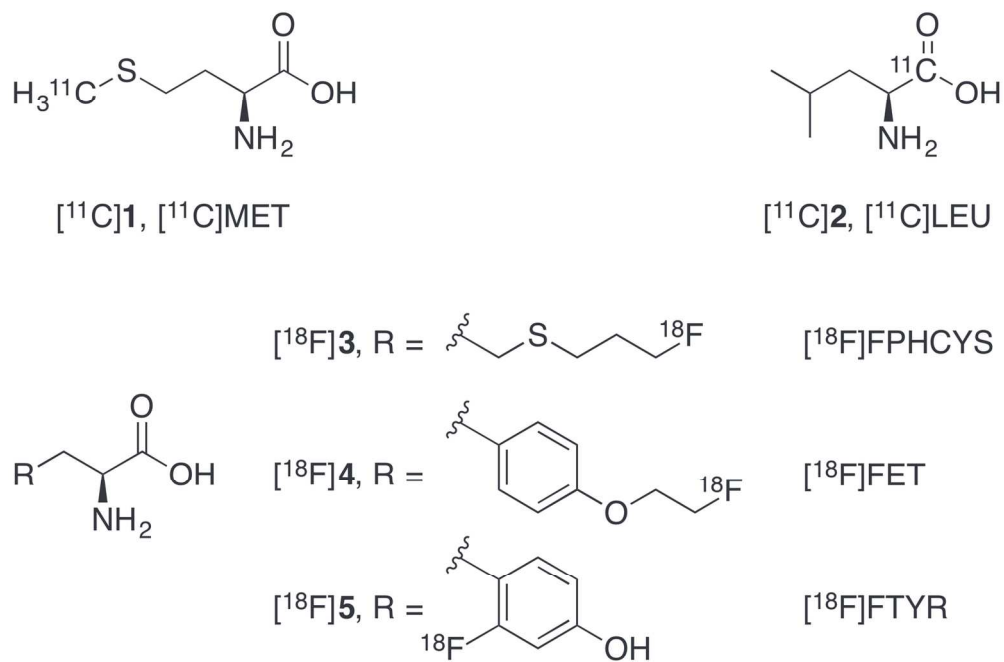
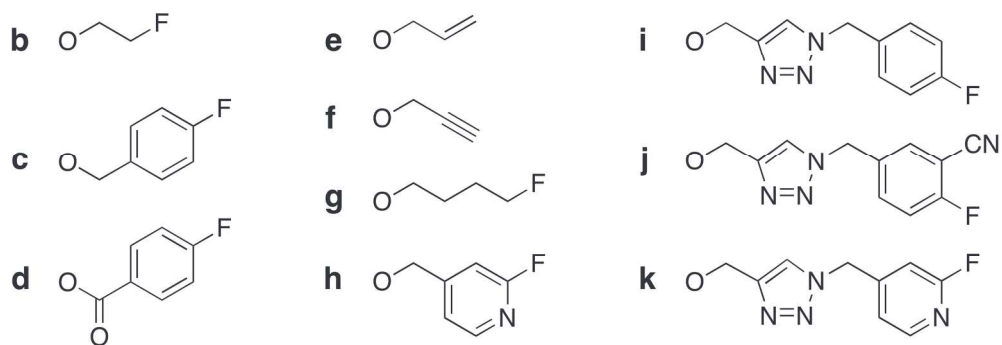
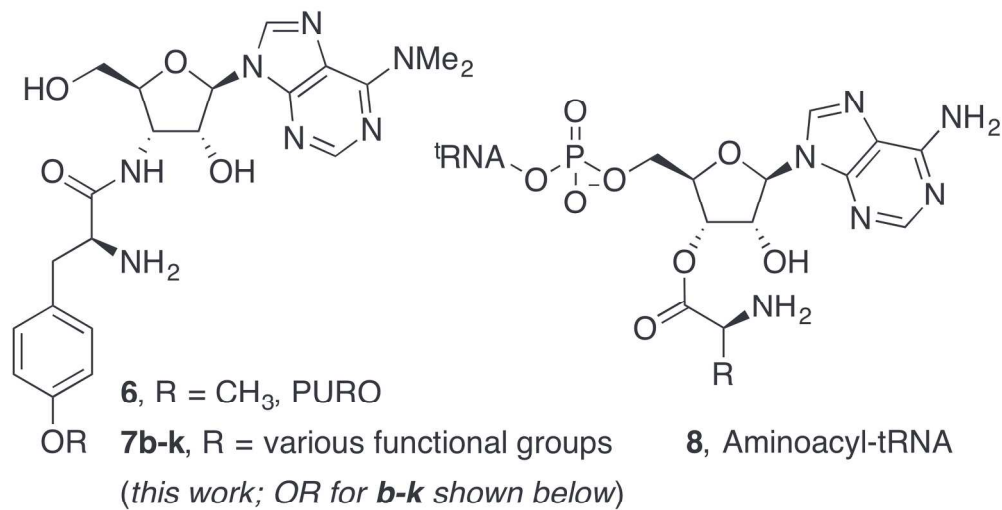


Figure 1. Selected carbon-11 and fluorine-18 amino acid radiotracers.

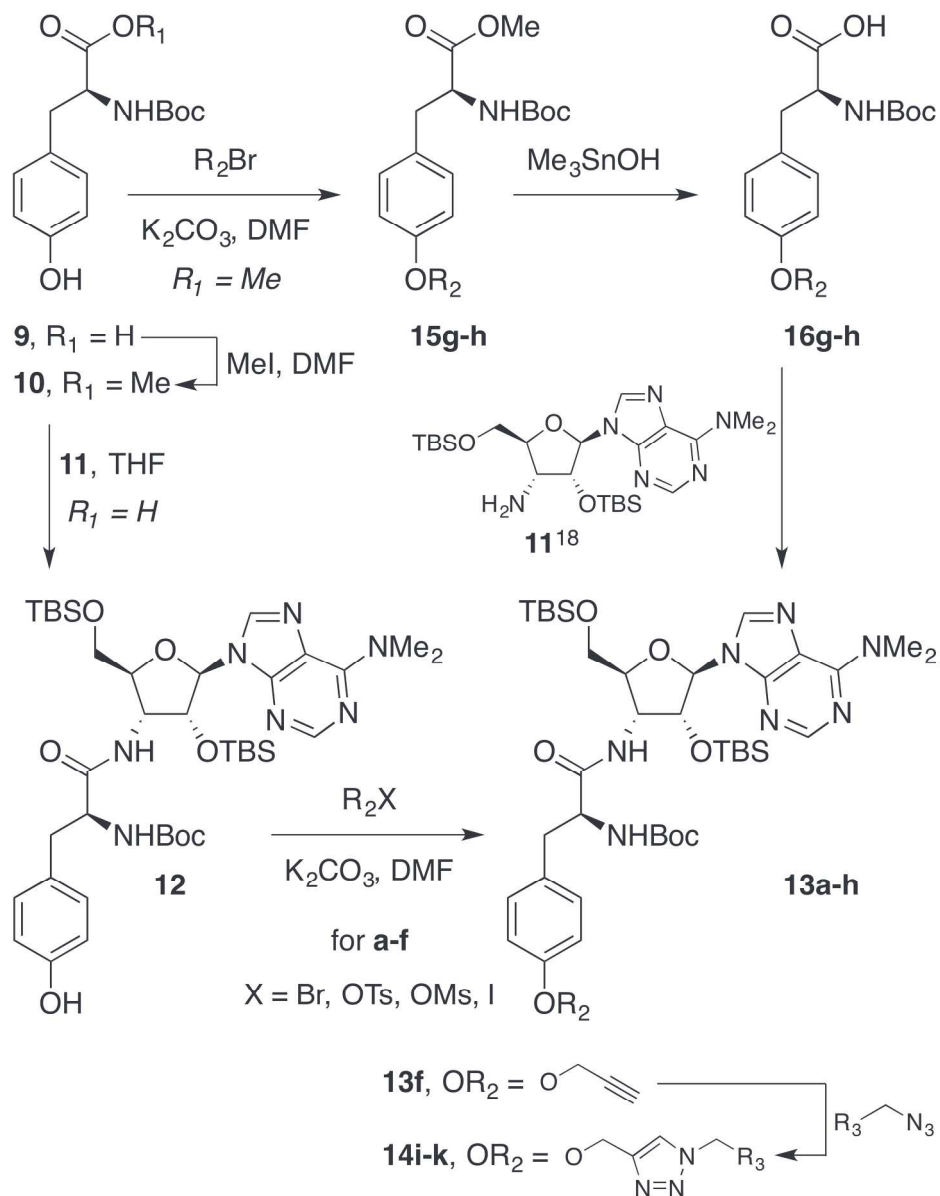
74x49mm (600 x 600 DPI)



37
38
39
40
41
42
43
44
45
46
47
48
49
50
51
52
53
54
55
56
57
58
59
60

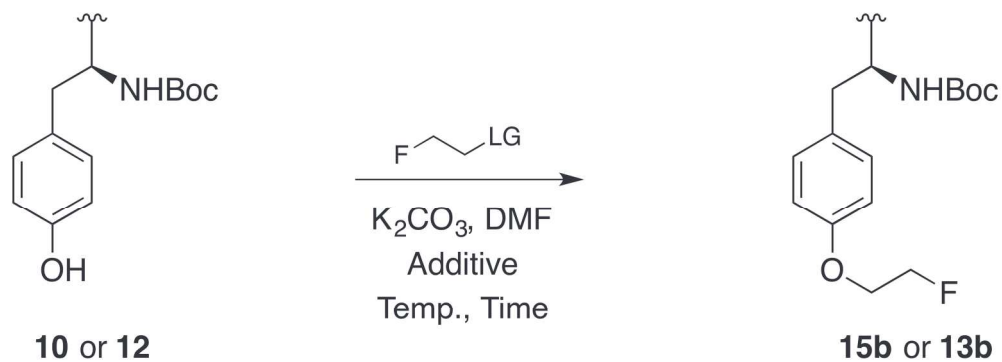
Figure 2. The structures of **6** (PURO), envisioned derivatives (**7**) and aminoacyl-tRNA (**8**).

100x90mm (600 x 600 DPI)



Scheme 1. Syntheses of TBS and Boc protected derivatives **7** and **14**, using direct and indirect Williamson ether methods (please refer to Supporting Information for respective yields).

144x184mm (600 x 600 DPI)



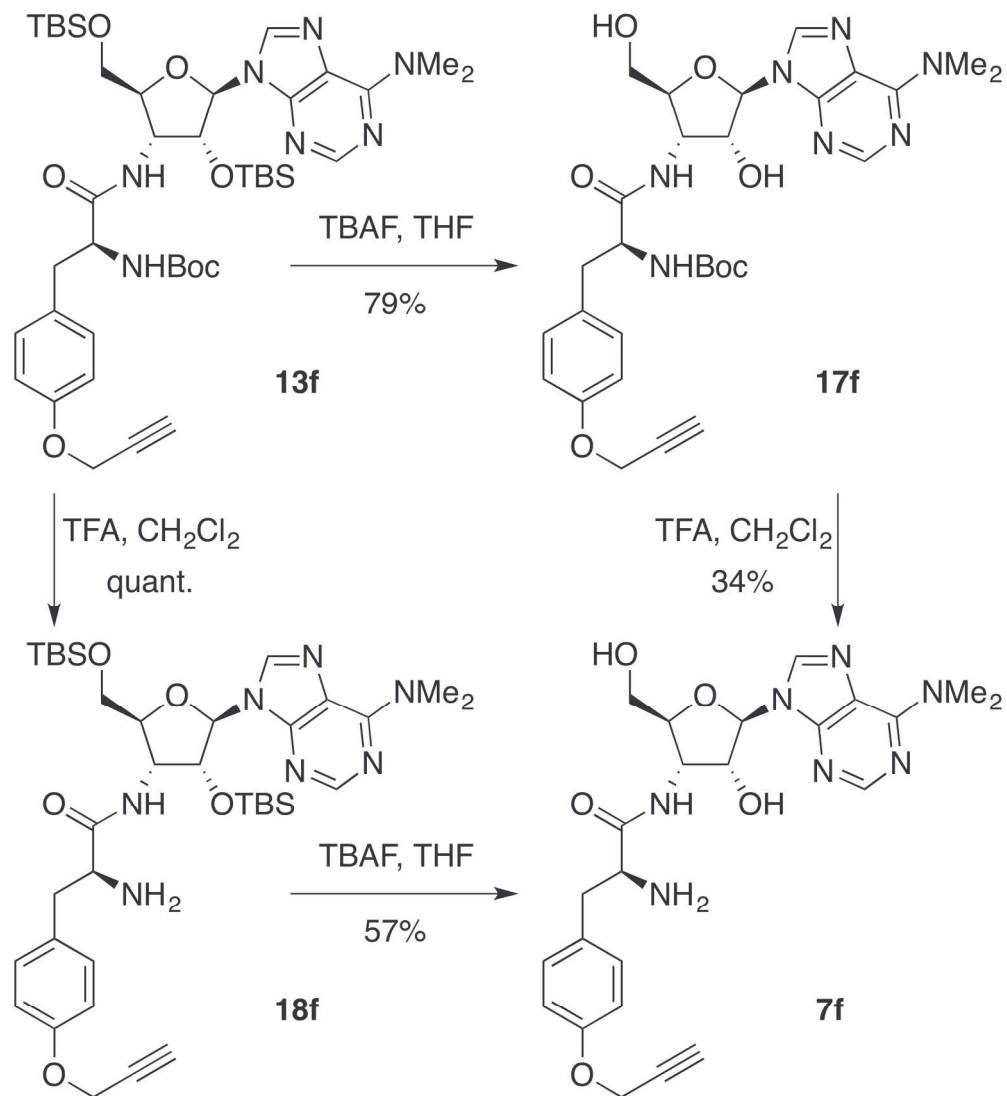
20
21
22
23
24
25
26
27
28
29
30
31
32
33
34
35
36

Entry	Phenol	LG	Temp. (°C)	Time (h)	Yield (%)	(S):(R)
1	12	OMs	23	25	16 ^a	—
2	12	OTs	23	19	trace	—
3	12	OTs	70	2	11	—
4	12	OTs	70	17	44	—
5	10	OMs	23	25	20 ^a	—
6	10	OTs	23	16	37 ^a	—
7	10	OTs	23	48	42 ^b	99:1
8	10	OTs	reflux	21	64 ^{b,c}	89:11

^a NMR conversion; ^b 18-c-6 used as additive; ^c MeCN was used as solvent

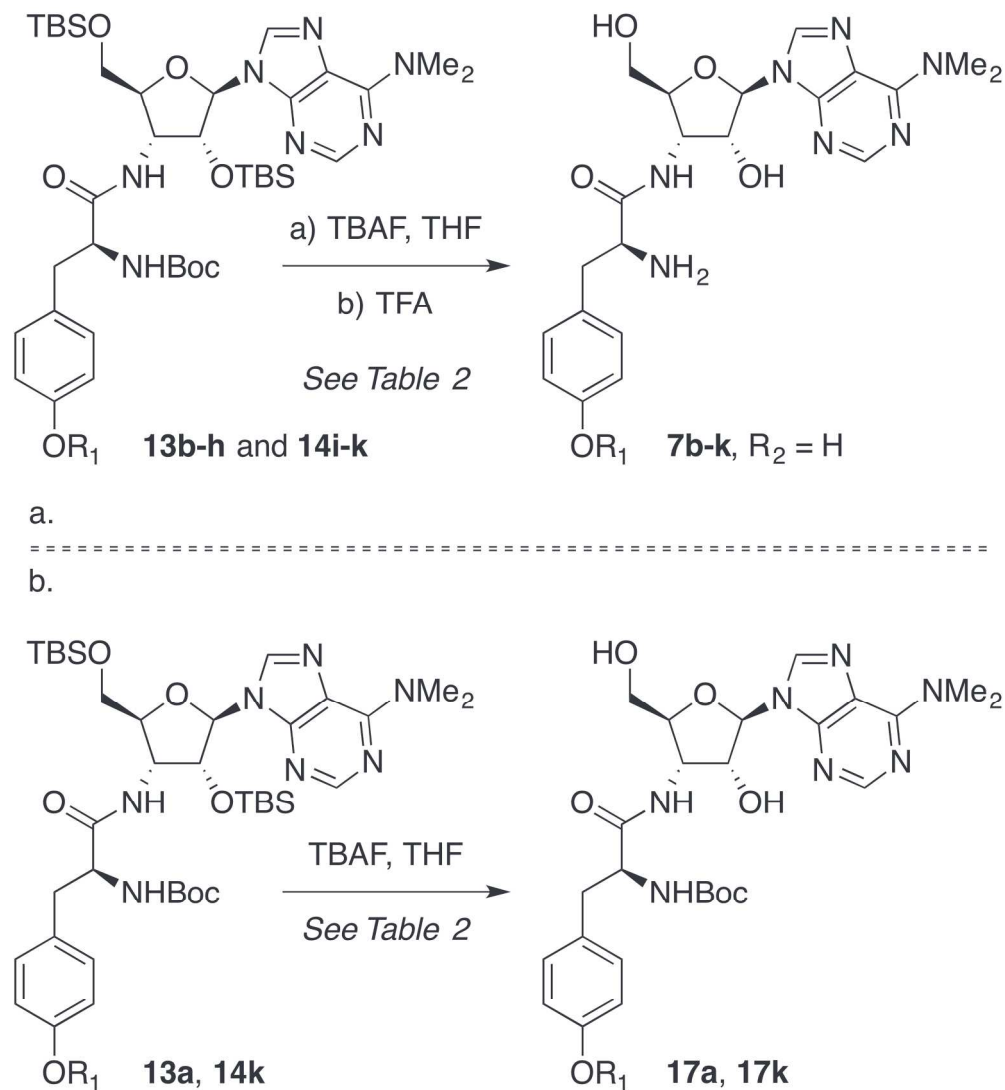
Table 1. Williamson ether synthesis with **10** and **12** and fluoroethyl electrophiles.

112x112mm (600 x 600 DPI)



Scheme 2. Two step deprotection of **13f** via two routes, yielding desired **7f** in structural agreement with the literature report.¹⁶

123x135mm (600 x 600 DPI)



Scheme 3. (a) Two step, one pot deprotection of TBS and Boc groups in **13/14** to afford derivatives **7**. (b) TBAF deprotection of TBS groups to obtain derivatives **17**.

122x133mm (600 x 600 DPI)

Entry	Derivative	OR ₁	Yield (%)	GLuc (%) ^a
1		OCH ₃	—	100
2			34 ^b	47
3			52	195
4			14	184
5			38	22
6			27	87
7			48	99
8			33	136
9			24	165
10			15	187
11			37	150
12		OR ₁ = OH, R ₂ = TBS	—	112
13		OR ₁ = OCH ₃ , R ₂ = TBS	—	192
14		OR ₁ = OCH ₃ , R ₂ = H	99	156
15		OR ₁ = , R ₂ = H	96	184
16		OR ₁ = , R ₂ = H	78 ^c	177

^a % GLuc production (vs. **6** inhibition) at 50 μM

^b Material was accessed via two different methods;

^c Material was prepared via [2 + 3] cycloaddition of azide directly with **17f**;

Please refer to Supporting information for details

Table 2. Structures of derivatives **7** and **17**, deprotection yields and inhibitory affinity data.

267x634mm (600 x 600 DPI)

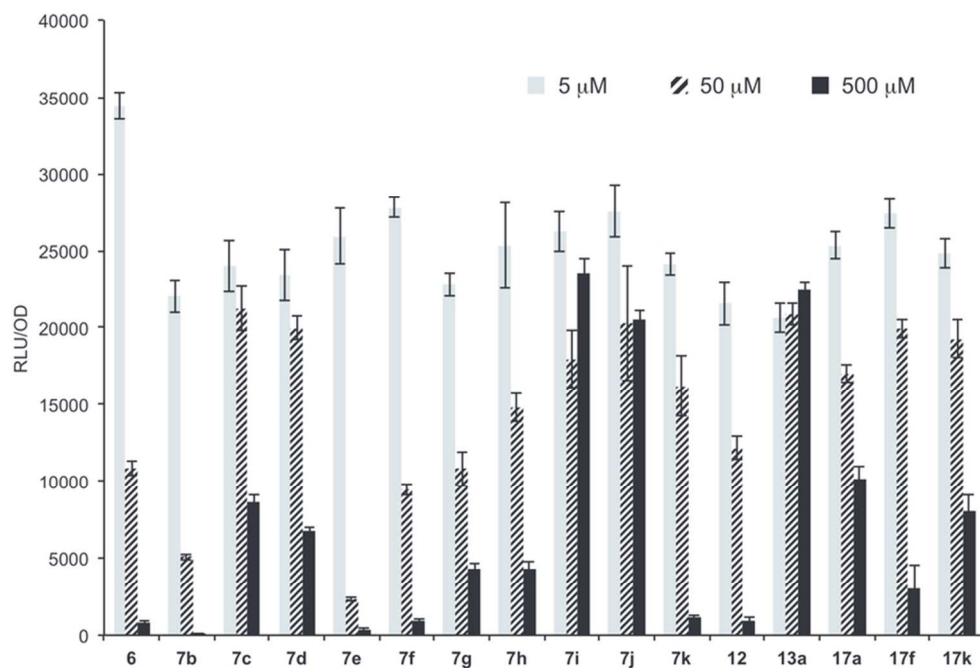
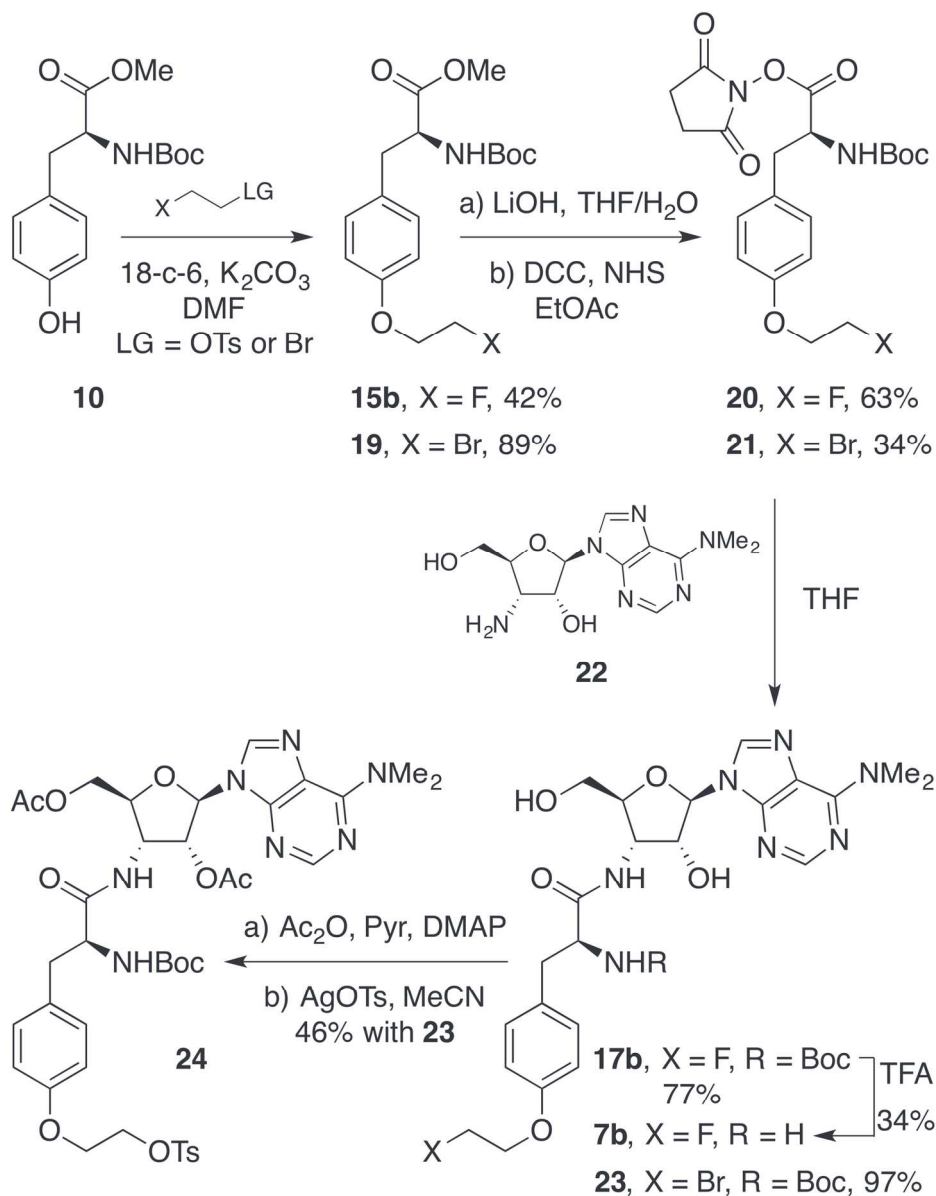
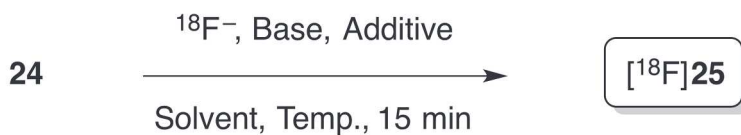


Figure 3. Effect of derivatives of **6** on protein synthesis, as indicated by inhibition of luciferase synthesis. RLU/OD = relative light units/optical density.

75x51mm (300 x 300 DPI)

Scheme 4. Synthesis of radiolabelling precursor **24** and revisited synthesis of **7b**.

144x185mm (300 x 300 DPI)

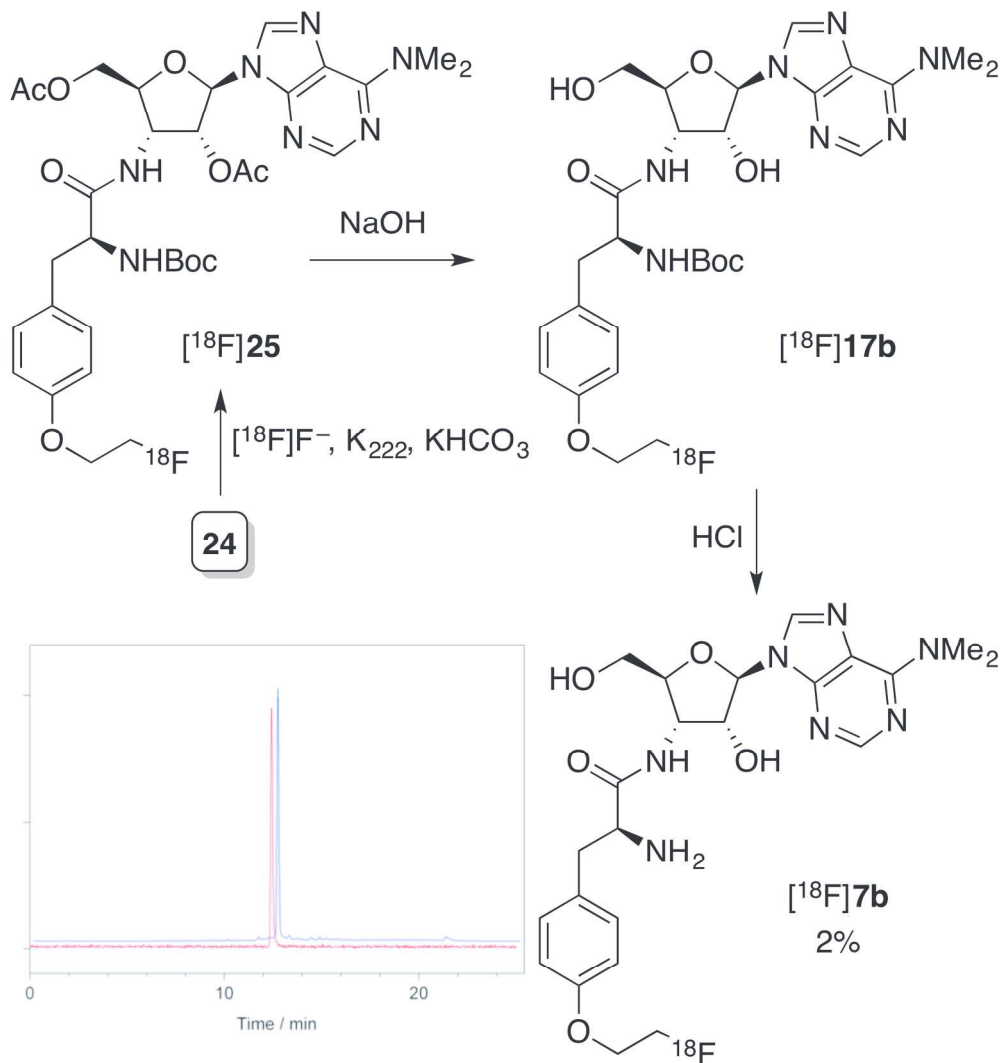


Entry	Base	Additive	Solvent	Temp. (°C)	HPLC conversion (%)
1	K ₂ CO ₃	K ₂₂₂	DMF	80	5
2	K ₂ CO ₃	K ₂₂₂	DMSO	80	13
3	K ₂ CO ₃	K ₂₂₂	MeCN	80	4
4	TBAHCO ₃	—	DMSO	80	12 ^a
5	KHCO ₃	K ₂₂₂	DMSO	80	18
6	KHCO ₃	K ₂₂₂	DMF	80	8
7	KHCO ₃	K ₂₂₂	DMSO	120	20 ^b
8	KHCO ₃	K ₂₂₂	DMSO	120	22
9	KHCO ₃	K ₂₂₂	DMSO	130	24 ^a
10	KHCO ₃	18-c-6	DMSO	120	0
11	KHCO ₃	K ₂₂₂	DMSO	120	12 ^{a,c}

^a Formation of by-products observed; ^b 10 min reaction time; ^c 7.5 mg of **24** used

Table 3. Optimisation of radiolabelling for preparation of [^{18}F]**25** from 10 mg of **24** (0.3 mL reaction volume).

109x107mm (600 x 600 DPI)



42
43
44
45
46
47
48
49
50
51
52
53
54
55
56
57
58
59
60

Radiosynthesis of $[^{18}\text{F}]\mathbf{7b}$ via nucleophilic substitution and deprotection. Overlaid radio (red) and UV (blue) HPLC traces of formulated $[^{18}\text{F}]\mathbf{7b}$, and $\mathbf{7b}$. Axes have been slightly offset for clarity.

120x128mm (600 x 600 DPI)

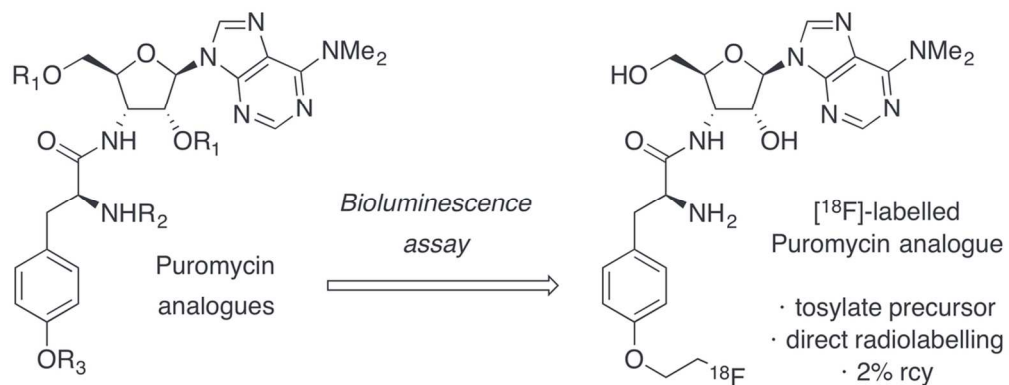


Table of Contents Graphic

53x20mm (600 x 600 DPI)